CP violation in B-hadrons

S. Benson
on behalf of the LHCb collaboration
CERN, Geneva, Switzerland.

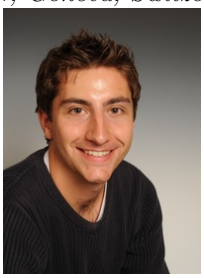

Latest LHCb measurements of *CP* violation in b-hadrons are presented based on *pp* collision data collected in 2011 and 2012 at centre-of-mass energies of $\sqrt{s} = 7\,\text{TeV}$ and $8\,\text{TeV}$, respectively. The total integrated luminosity collected is $3.0\,fb^{-1}$. Results include recent measurements of *CP* violation in B^0 and B^0_s mixing, along with those of quantifying the effects of $b \to c\bar{c}s$ loop pollution. Standard Model *CP* violation tests in loop transitions are discussed with results consistent with expectations. New decays of b-baryons are presented and preliminary studies of *CP* violation are performed.

1 Overview of *CP* violation

In the Standard Model (SM), *CP* violation is governed by the Cabibbo-Kobayashi-Maskawa (CKM) mechanism. The most common way of depicting the global fit to the four free parameters is via the CKM triangle in the $\bar{\eta}$-$\bar{\rho}$ plane, where $\bar{\eta}$ and $\bar{\rho}$ are Wolfenstein parameters. The current CKM global fit in this plane is presented in Fig. 1, where the effect of individual observables is shown (see Ref. 1 for a detailed description of the inputs). At LHCb, $J/\psi \to \mu\mu$ decays are selected with high efficiency. The relatively high branching fraction of decays such as $B^0_s \to J/\psi\,\phi$ and $B^0 \to J/\psi\,K^0_S$ gives large samples of $b \to c\bar{c}s$ decays and enables LHCb to provide important inputs to *CP* violation in the interference between neutral meson mixing and decay. The observable measured is the time-dependent *CP* asymmetry, defined as

$$\mathcal{A}_q(t) \equiv \frac{\Gamma(\overline{B}^0_q(t) \to J/\psi\,X_q) - \Gamma(B^0_q(t) \to J/\psi\,X_q)}{\Gamma(\overline{B}^0_q(t) \to J/\psi\,X_q) + \Gamma(B^0_q(t) \to J/\psi\,X_q)} = \frac{S_q \sin(\Delta m_q\,t) - C_q \cos(\Delta m_q\,t)}{\cosh(\frac{\Delta\Gamma_q\,t}{2}) + A_{\Delta\Gamma_q} \sinh(\frac{\Delta\Gamma_q\,t}{2})}, \quad (1)$$

where X_s indicates an $(\bar{s}s)$ state and X_d an $(\bar{s}d)$ state; t indicates the decay time. The parameters Δm_q and $\Delta\Gamma_q$ are the mass and the decay width differences between the heavy and light mass eigenstates of the B^0_q-$\overline{B}^0_q$ system, and S_q, C_q, and $A_{\Delta\Gamma_q}$ are *CP* observables. The *CP* observable, $S_q \equiv \sin(-2\beta_q) = \sin(\phi_q^{c\bar{c}s})$ is the most sensitive to $\phi_q^{c\bar{c}s}$. The angle β_q is related to CKM matrix elements through the relation $\beta_q \equiv \arg[-(V_{cq}V^*_{cb})/(V_{tq}V^*_{tb})]$. The time-dependent *CP* asymmetry has recently been measured by LHCb in $B^0 \to J/\psi\,K^0_S$ decays [2]. The distribution of $\mathcal{A}_d(t)$ as a

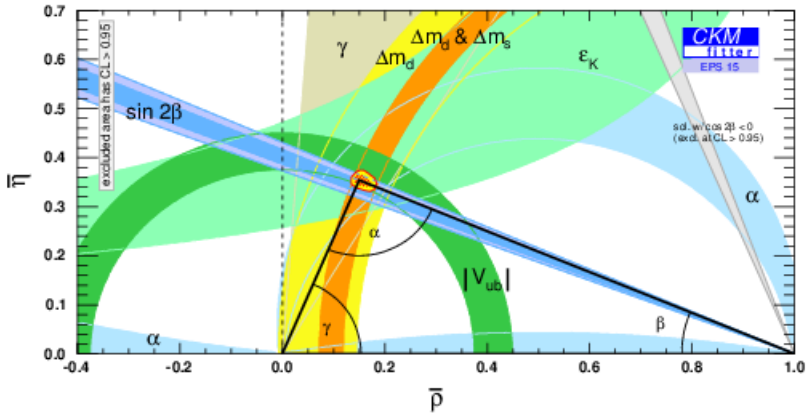

Figure 1 – Current picture of the CKM global fit in the η-ρ plane [1].

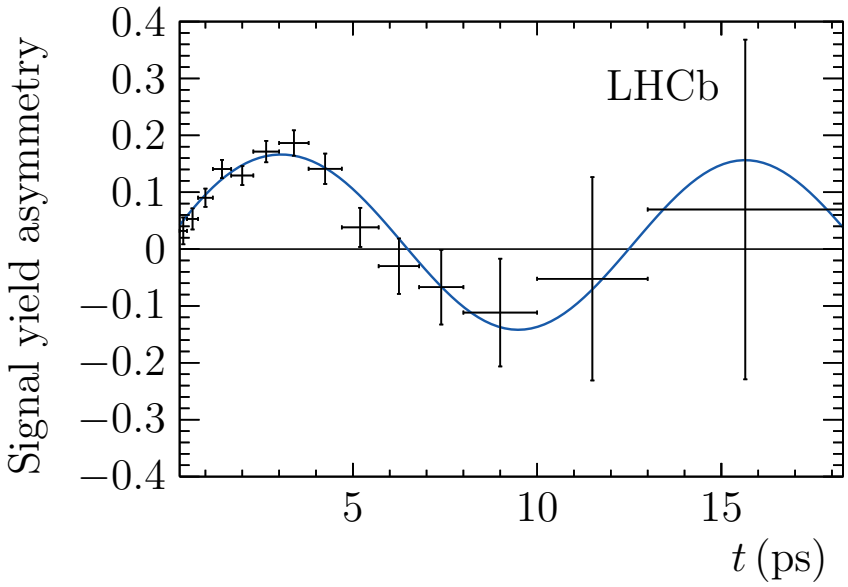

Figure 2 – Raw *CP* asymmetry as a function of decay time obtained from $B^0 \to \mathrm{J}/\psi \mathrm{K}^0_\mathrm{S}$ decays[2].

function of decay time for candidates is shown in Fig. 2. The results of a maximum likelihood fit including the effects of flavour tagging result in a value of $\sin(2\beta_d) = 0.731 \pm 0.035\,(\mathrm{stat}) \pm 0.020\,(\mathrm{syst})$, which is consistent with measurements from the B-factories and comparable in precision. The largest systematic uncertainty on the measurement of $\sin(2\beta_d)$ arises from possible flavour asymmetries in the background candidates. The comparison of the LHCb result against those of the B-factories, CDF and LEP experiments is given in Fig. 3, along with the combination provided by HFAG [3].

The corresponding *CP* observables in the B^0_s system are measured in decays that are not pure *CP* eigenstates. This provides an extra complication as an angular analysis in the helicity basis is performed to disentangle the *CP* eigenstates. The SM prediction for $\phi_\mathrm{s}^{c\bar{c}\mathrm{s}}$ is obtained from global fits to experimental data yielding a value of -0.036 ± 0.002 rad [7,8,9]. There are however many BSM theories that provide additional contributions to B^0_s mixing diagrams that alter this value [10,11]. The most recent LHCb measurement of $\phi_\mathrm{s}^{c\bar{c}\mathrm{s}}$ is performed using a combination of $B^0_\mathrm{s} \to \mathrm{J}/\psi \mathrm{K}^+\mathrm{K}^-$ and $B^0_\mathrm{s} \to \mathrm{J}/\psi \pi^+\pi^-$ decays, yielding a value of $\phi_\mathrm{s}^{c\bar{c}\mathrm{s}} = 0.010 \pm 0.039\,\mathrm{rad}$[4]. The result can be seen to dominate the world average, shown in Fig. 4.

Experimentally, measurements of the *CP*-violating phases in B mixing are affected by loop

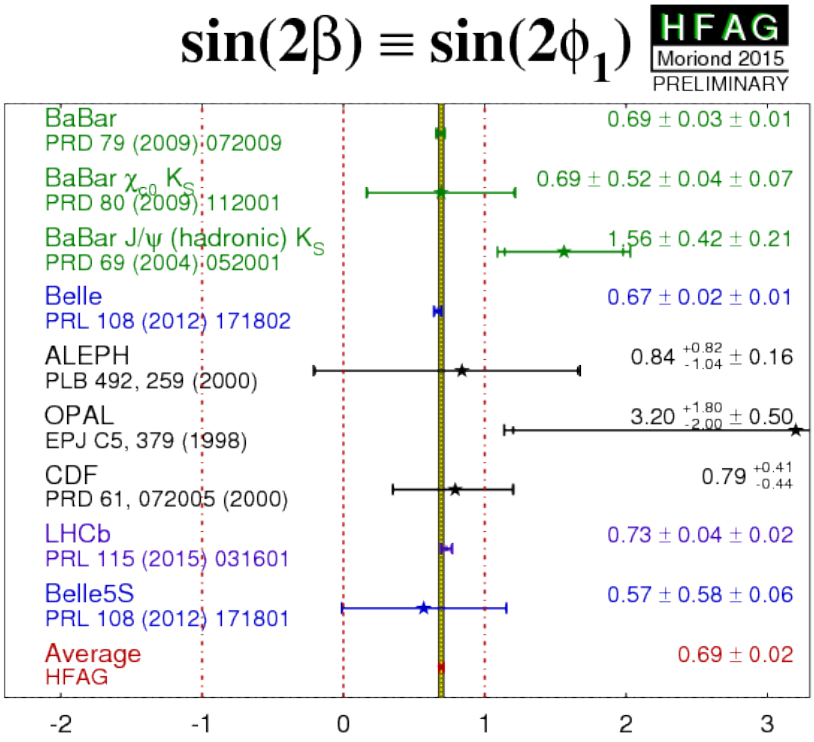

Figure 3 – Experimental measurements of the CKM angle β along with the world average as performed by the Heavy Flavour Averaging Group [3].

topologies, causing the measured value to be polluted. The effect of loop topologies or so-called penguin pollution is determined through the analysis of decay modes related via $SU(3)$ flavour symmetry [13], in which the penguin contribution is not suppressed. For the case of B^0_s-$\overline{B}^0_s$ mixing, one such decay mode is $B^0_s \to J/\psi \overline{K}^{*0}$ [14 a]. When decomposed into its different sources, the angle $\phi_s^{c\bar{c}s}$ takes the form

$$\phi_s^{c\bar{c}s} = -2\beta_s + \phi_s^{\rm BSM} + \Delta\phi_s^{J/\psi\,\phi}, \tag{2}$$

where $-2\beta_s$ is the SM contribution, $\phi_s^{\rm BSM}$ is a possible beyond the SM phase, and $\Delta\phi_s^{J/\psi\,\phi}$ is a shift introduced by the presence of penguin pollution. The transition amplitude for the $B^0_s \to J/\psi \overline{K}^{*0}$ decay may be written as

$$A\left(B^0_s \to (J/\psi \overline{K}^{*0})_i\right) = -\lambda \mathcal{A}_i \left[1 - a_i e^{i\theta_i} e^{i\gamma}\right] \tag{3}$$

where $\lambda = |V_{us}|$ and i labels the different polarisation states. In eq. 3, $\mathcal{A}_i$ is a CP-conserving hadronic matrix element that represents the tree topology, and a_i parametrises the relative contribution from the penguin topologies. The CP-conserving phase difference between the two terms is parametrised by θ_i, whereas their weak phase difference is given by the CKM angle γ. The branching fraction, the CP asymmetries, and the polarisation fractions of the $B^0_s \to J/\psi \overline{K}^{*0}$ decay depend on the penguin parameters a_i and θ_i.

The transition amplitude for the $B^0_s \to J/\psi\,\phi$ decay can be written as

$$A\left(B^0_s \to (J/\psi\,\phi)_i\right) = \left(1 - \frac{\lambda^2}{2}\right) \mathcal{A}'_i \left[1 + \epsilon a'_i e^{i\theta'_i} e^{i\gamma}\right], \tag{4}$$

[a] Similar studies have also been undertaken in the study of B^0-$\overline{B}^0$ mixing, most recently using the $B^0_s \to J/\psi\,K^0_S$ decay channel [12].

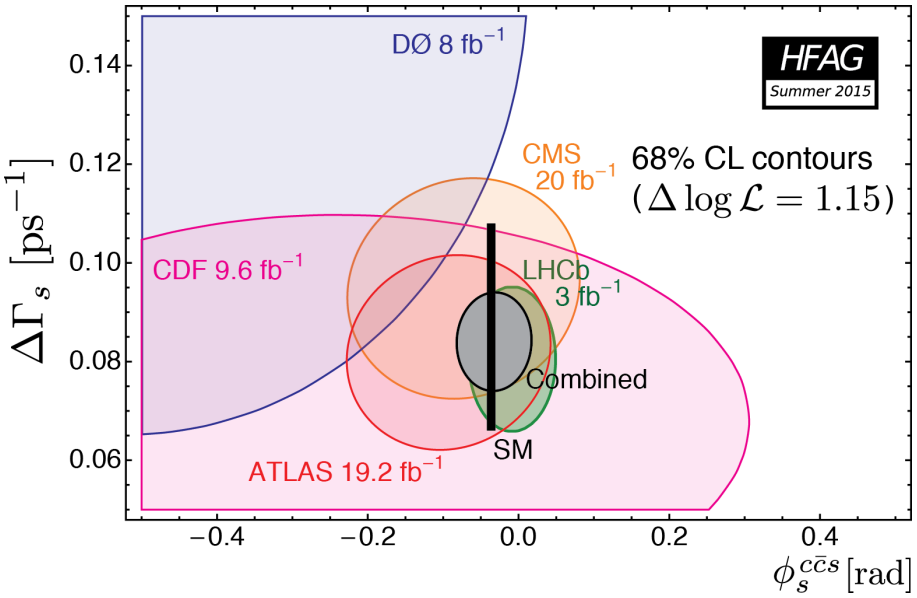

Figure 4 – The two-dimensional 68% confidence level contours of $\Delta\Gamma_s$ vs. $\phi_s^{c\bar{c}s}$ from the LHC and the Tevatron, along with the combination[3] compared to theoretical predictions.

where the penguin parameters a_i' and θ_i' are defined in analogy to a_i and θ_i. Assuming $SU(3)$ flavour symmetry, and neglecting contributions from exchange and penguin-annihilation topologies, $a_i' = a_i$ and $\theta_i' = \theta_i$. The penguin parameters a_i and θ_i are found from their relations to the branching fractions and CP asymmetries in the three polarisation states. These can then be used to determine the CP phase pollution using external CKM inputs on γ and λ. The phase shift is calculated to be

$$\begin{aligned}
\Delta\phi_{s,0}^{\mathrm{J}/\psi\,\phi} &= \quad 0.003 \;{}^{+0.084}_{-0.011}\,(\mathrm{stat})\;{}^{+0.014}_{-0.009}\,(\mathrm{syst})\;{}^{+0.047}_{-0.030}\,(|\mathcal{A}_i'/\mathcal{A}_i|),\\
\Delta\phi_{s,\parallel}^{\mathrm{J}/\psi\,\phi} &= \quad 0.031 \;{}^{+0.047}_{-0.037}\,(\mathrm{stat})\;{}^{+0.010}_{-0.013}\,(\mathrm{syst})\pm 0.032\,(|\mathcal{A}_i'/\mathcal{A}_i|),\\
\Delta\phi_{s,\perp}^{\mathrm{J}/\psi\,\phi} &= -0.045\pm 0.012\,(\mathrm{stat})\pm 0.008\,(\mathrm{syst})\;{}^{+0.017}_{-0.024}\,(|\mathcal{A}_i'/\mathcal{A}_i|).
\end{aligned}$$

These limits are improved with a combined analysis using the additional input from an earlier analysis of the $B^0 \to \mathrm{J}/\psi\,\rho$ decay [15], which then gives phase shifts of

$$\begin{aligned}
\Delta\phi_{s,0}^{\mathrm{J}/\psi\,\phi} &= 0.000^{+0.009}_{-0.011}\,(\mathrm{stat})\;{}^{+0.004}_{-0.009}\,(\mathrm{syst})\,\mathrm{rad},\\
\Delta\phi_{s,\parallel}^{\mathrm{J}/\psi\,\phi} &= 0.001^{+0.010}_{-0.014}\,(\mathrm{stat})\pm 0.008\,(\mathrm{syst})\,\mathrm{rad},\\
\Delta\phi_{s,\perp}^{\mathrm{J}/\psi\,\phi} &= 0.003^{+0.010}_{-0.014}\,(\mathrm{stat})\pm 0.008\,(\mathrm{syst})\,\mathrm{rad}.
\end{aligned}$$

The effect of $SU(3)$ breaking is found to be small. The results show that the penguin phase shift is consistent with zero in all polarisations. This then means that at the current level of precision, there is no significant level of penguin pollution, and with increased dataset sizes, the control of penguin pollution can be determined using data-driven methods.

2 BSM searches in loop B-decays

In addition to being sources of pollution to other measurements, penguin loops offer tests of the SM, provided the theoretical expectations are understood. The CP-violating phase in the SM is predicted to be close to zero for the cases of $\mathrm{b} \to \mathrm{s\bar{s}s}$ and $\mathrm{b} \to \mathrm{sd\bar{d}}$ flavour changing neutral current (FCNC) transitions [17]. This makes CP violation searches with decays such as $B_\mathrm{s}^0 \to \phi\phi$ and $B_\mathrm{s}^0 \to \mathrm{K}^{*0}\overline{\mathrm{K}}^{*0}$ important null tests of the SM. In addition, the polarisation structure of

Table 1: Results of the $B_s^0 \to K^{*0}\overline{K}^{*0}$ angular fit [16] (phases are measured in radians). The first uncertainties are statistical and the second systematic.

Parameter	Value
f_L	$0.201 \pm 0.057 \pm 0.040$
$f_\parallel$	$0.215 \pm 0.046 \pm 0.015$
$\lvert A_s^+\rvert^2$	$0.114 \pm 0.037 \pm 0.023$
$\lvert A_s^-\rvert^2$	$0.485 \pm 0.051 \pm 0.019$
$\lvert A_{ss}\rvert^2$	$0.066 \pm 0.022 \pm 0.007$
$\delta_\parallel$	$5.31 \pm 0.24 \pm 0.14$
$\delta_\perp - \delta_s^+$	$1.95 \pm 0.21 \pm 0.04$
δ_s^-	$1.79 \pm 0.19 \pm 0.19$
δ_{ss}	$1.06 \pm 0.27 \pm 0.23$

such pseudoscalar to vector-vector ($P \to VV$) decays provides not only tests of the predictions of QCD factorisation in the measurement of the polarisation fractions [17,18], but also gives rise to T-odd observables that can probe CP violation without the need for flavour-tagging or the resolution of B_s^0-$\overline{B}_s^0$ oscillations [19,20]. Most recently, the $B_s^0 \to K^{*0}\overline{K}^{*0}$ decay channel has been used to perform such tests in FCNC transitions, using $1.0\, fb^{-1}$ of 7 TeV data collected in 2011 [16]. As an example of a pseudoscalar to vector-vector ($P \to VV$) decay, the final state is a mixture of CP eigenstates. This can be described by three polarisation amplitudes in the helicity basis (A_0, $A_\perp$, $A_\parallel$). The Kπ final state is known to contain a significant scalar (S) contribution, which can also be described by the addition of three amplitudes (A_{VS}, A_{SV}, A_{SS}). The contributions involving a single scalar Kπ contribution can be re-parameterised as

$$A_s^+ = \frac{1}{\sqrt{2}}\left(A_{VS} + A_{SV}\right) \quad \text{and} \quad A_s^- = \frac{1}{\sqrt{2}}\left(A_{VS} - A_{SV}\right), \tag{5}$$

such that the total decay rate is expressed in CP-even and CP-odd terms. The final decay rate consists of 21 terms. The determination of the polarisation fractions (f_L, $f_\parallel$, $|A_s^+|^2$, $|A_s^-|^2$, $|A_{ss}|^2$) and the strong phase differences between the polarisations ($\delta_\parallel$, $\delta_\perp - \delta_s^+$, δ_s^-, δ_{ss}) consists of a maximum likelihood fit to the decay angles and the Kπ invariant masses. The results of the angular fit are shown in Table 1. The relatively small value of f_L is consistent with that reported in other FCNC b $\to$ s transitions, most notably the $B_s^0 \to \phi\phi$ decay, where LHCb has reported a longitudinal polarisation fraction of $0.364 \pm 0.012\,(\text{stat}) \pm 0.009\,(\text{syst})$ [21].

In the decay rate, the coefficients $\Im(A_\perp A_{0,\parallel}^* - \bar{A}_\perp \bar{A}_{0,\parallel}^*)$ and $\Im[(\bar{A}_\perp A_{0,\parallel}^* + A_\perp^* \bar{A}_{0,\parallel})e^{-i\phi_s^{c\bar{c}s}}]$ are T-odd observables. The decay-time-integrated coefficients summed over B_s^0 and $\overline{B}_s^0$ decays correspond to triple product asymmetries that probe CP violation. The interference with the longitudinal and parallel polarisation is denoted by A_T^1 and A_T^2, respectively. When the spin-0 contribution is taken into account, two additional CP-even amplitudes, $\mathcal{A}_s^-(t)$ and $\mathcal{A}_{SS}(t)$, interfere with $\mathcal{A}_\perp(t)$, and give rise to two additional CP-violating terms, denoted as A_T^3 and A_T^4, respectively. Since $\mathcal{A}_s^+(t)$ is also CP-odd, its interference terms with the CP-even amplitudes also give rise to CP violating asymmetries. These take the form $\Re(\mathcal{A}_s^+(t)\mathcal{A}_k^*(t) - \bar{\mathcal{A}}_s^+(t)\bar{\mathcal{A}}_k^*(t))$, with $k = 0, \parallel, s^-, ss$, and are denoted by $A_D^{1,2,3,4}$. Each triple product asymmetry is accessed through angular observables that isolate the corresponding coefficient. The results of the CP violation measurements are given in Table 2 and are consistent with CP conservation although uncertainties are relatively large. The observance of CP conservation is consistent with that reported in $B_s^0 \to \phi\phi$ decays, in which the weak phase was found to be $0.17 \pm 0.15\,(\text{stat}) \pm 0.03\,(\text{syst})\,\text{rad}$ [21].

Table 2: Triple product and direct *CP* asymmetries measured in $B_s^0 \to K^{*0}\overline{K}^{*0}$ decays [16]. The first uncertainties are statistical and the second systematic.

Asymmetry	Value
A_T^1	$0.003 \pm 0.041 \pm 0.009$
A_T^2	$0.009 \pm 0.041 \pm 0.009$
A_T^3	$0.019 \pm 0.041 \pm 0.008$
A_T^4	$-0.040 \pm 0.041 \pm 0.008$
A_D^1	$-0.061 \pm 0.041 \pm 0.012$
A_D^2	$0.081 \pm 0.041 \pm 0.008$
A_D^3	$-0.079 \pm 0.041 \pm 0.023$
A_D^4	$-0.081 \pm 0.041 \pm 0.010$

3 Searches and CPV studies in b-baryon decays

The vast majority of *CP* violation measurements in beauty decay have focused on B mesons due to the rich phenomenology available in meson mixing and the large datasets collected by the B-factories. The LHC also produces beauty in the form of Λ_b^0 baryons at the level of $\sim 1/9$ that of B^0 mesons [22], which gives large samples of Λ_b^0 baryons for *CP* measurements.

At LHCb, dataset sizes have allowed for searches of loop transitions with suppressed branching fractions. An example of a $b \to s\bar{s}s$ transition in the baryonic sector is the $\Lambda_b^0 \to \Lambda\phi$ decay. A recent analysis of the decay has been performed using $3.0\,fb^{-1}$ of LHCb data [23]. Due to the long-lived nature of the Λ baryon, the dataset is split according to whether the Λ baryon decayed inside or outside the vertex locator. This then allows for the different selection efficiencies and resolutions to be accounted for. The approach taken is to fit in the three invariant mass dimensions ($M_{K^+K^-p\pi^-}$, $M_{K^+K^-}$, $M_{p\pi^-}$). The projection on to each dimension split according to long and downstream categories is shown in Fig. 5. The mass fit results in a yield of 89 ± 13. On the inclusion of systematic uncertainties, the significance is calculated to be 5.9 standard deviations representing a first observation. In order to calculate the branching fraction, the $B^0 \to K_S^0\phi$ decay is used as a control mode due to the similarity both in terms of selection requirements and the presence of a long-lived resonance. The value of the branching fraction is then measured to be $(5.18 \pm 1.04 \pm 0.35\,^{+0.67}_{-0.62}) \times 10^{-6}$, where the first uncertainty is statistical, the second is systematic, and the third is related to external inputs. Triple product asymmetries can also be computed in the $\Lambda_b^0 \to \Lambda\phi$ decay due to the spin structure of the decay. These have been performed following the formalism of Leitner and Ajaltouni [24]. Four triple products are possible, corresponding to $\cos\Phi_{n_{\Lambda,\phi}}$ and $\sin\Phi_{n_{\Lambda\phi}}$ observables, which are azimuthal angles of the resonance decay planes (with normal vector $\vec{n}_{\Lambda,\phi}$). The asymmetries $A_\Lambda^{c,s}$ and $A_\phi^{c,s}$, where c and s correspond to the cosine and sine respectively, are determined experimentally through a simultaneous unbinned maximum likelihood fit to datasets in which the relevant observables are positive and negative. The results are determined to be

$$\begin{aligned}
A_\Lambda^c &= -0.22 \pm 0.12\,(\text{stat}) \pm 0.06\,(\text{syst}),\\
A_\Lambda^s &= 0.13 \pm 0.12\,(\text{stat}) \pm 0.05\,(\text{syst}),\\
A_\phi^c &= -0.01 \pm 0.12\,(\text{stat}) \pm 0.03\,(\text{syst}),\\
A_\phi^s &= -0.07 \pm 0.12\,(\text{stat}) \pm 0.01\,(\text{syst}),
\end{aligned}$$

where systematic contributions mainly arise from the mass model.

In addition to the exclusive $\Lambda_b^0 \to \Lambda\phi$ search, an inclusive measurement of $\Lambda_b^0 \to \Lambda hh'$ decays, where $h, h' \in \{K, \pi\}$, has been performed using $3.0\,fb^{-1}$ of LHCb data [25]. The analysis uses the abundant $\Lambda_b^0 \to \Lambda_c^+\pi^-$ control mode. The result of the maximum likelihood mass fit is shown in Fig. 6. The statistical significance is found to be 5.2 standard deviations for the case of the $\Lambda_b^0 \to \Lambda K^+K^-$ decay, 8.5 for the $\Lambda_b^0 \to \Lambda K^+\pi^-$ decay, and 20.5 for the $\Lambda_b^0 \to \Lambda K^+K^-$ decay.

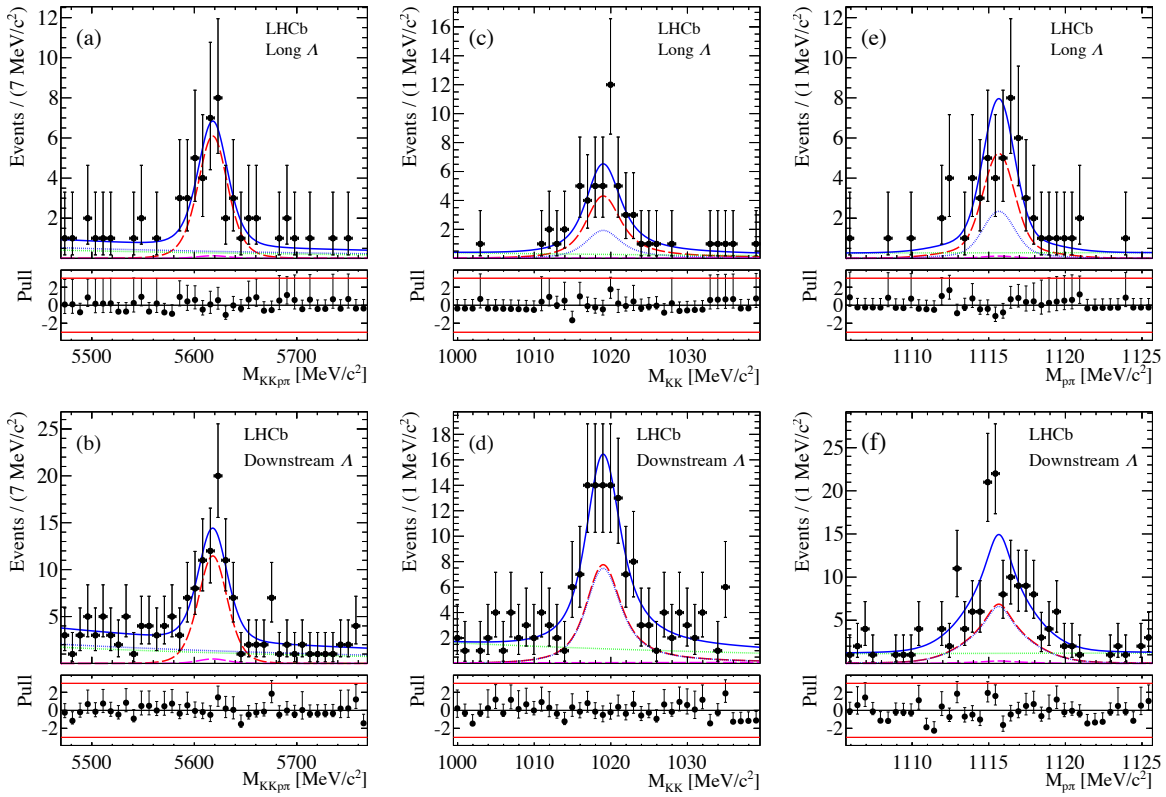

Figure 5 – Fit projections to the $\mathrm{K}^+\mathrm{K}^-p\pi^-$ invariant mass in the (a) long and (b) downstream datasets, the $\mathrm{K}^+\mathrm{K}^-$invariant mass in the (c) long and (d) downstream datasets, and the $p\pi^-$invariant mass in the (e) long and (f) downstream datasets. The total fit projection is given by the blue solid line. The blue and green dotted lines represent the $\phi + \Lambda$ and pure combinatorial fit components, respectively. The red and magenta dashed lines represent the $\Lambda_\mathrm{b}^0 \to \Lambda\phi$ signal and the $\Lambda_\mathrm{b}^0 \to \Lambda\mathrm{K}^+\mathrm{K}^-$ non-resonant components, respectively. Black points represent the data. Data uncertainties are Poisson 68% confidence intervals.

No Ξ_b^0 decay evidence is seen. Although the statistical significance of the $\Lambda_\mathrm{b}^0 \to \Lambda\pi^+\pi^-$ channel is over 5 standard deviations, the systematic uncertainty reduces the significance of the channel to evidence. The branching fractions are measured to be

$$\begin{aligned}
\mathcal{B}(\Lambda_\mathrm{b}^0 \to \Lambda\pi^+\pi^-) &= (4.6 \pm 1.2 \pm 1.4 \pm 0.6) \times 10^{-6}, \\
\mathcal{B}(\Lambda_\mathrm{b}^0 \to \Lambda\mathrm{K}^+\pi^-) &= (5.6 \pm 0.8 \pm 0.8 \pm 0.7) \times 10^{-6}, \\
\mathcal{B}(\Lambda_\mathrm{b}^0 \to \Lambda\mathrm{K}^+\mathrm{K}^-) &= (15.9 \pm 1.2 \pm 1.2 \pm 2.0) \times 10^{-6},
\end{aligned}$$

where the last quoted uncertainty is due to the precision with which the normalisation channel branching fraction is known. The significant yields observed in the $\Lambda_\mathrm{b}^0 \to \Lambda\mathrm{K}^+\mathrm{K}^-$ and $\Lambda_\mathrm{b}^0 \to \Lambda\mathrm{K}^+\mathrm{K}^-$ decays allows for the determination of phase-space-integrated *CP* asymmetries, which are found to be

$$\begin{aligned}
\mathcal{A}_{CP}(\Lambda_\mathrm{b}^0 \to \Lambda\mathrm{K}^+\pi^-) &= -0.53 \pm 0.23 \pm 0.11, \\
\mathcal{A}_{CP}(\Lambda_\mathrm{b}^0 \to \Lambda\mathrm{K}^+\mathrm{K}^-) &= -0.28 \pm 0.10 \pm 0.07,
\end{aligned}$$

and are therefore consistent with *CP* conservation, though will be interesting with larger dataset sizes.

4 Summary

Measurements of the *CP*-violating phases in B^0 and B_s^0 mixing have been presented, along with measurements of the effects of penguin pollution in the latter. Results are consistent with SM

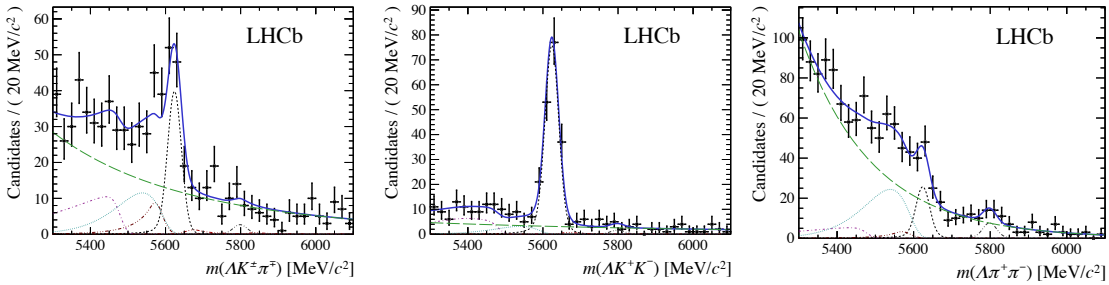

Figure 6 – Results of the fit for the (left) $\Lambda K^{\pm}\pi^{\mp}$, (middle) $\Lambda K^{+}K^{-}$ and (right) $\Lambda\pi^{+}\pi^{-}$ final states for all subsamples combined. Superimposed on the data are the total result of the fit as a solid blue line, the Λ_b^0 (Ξ_b^0) decay as a short-dashed black (double dot-dashed grey) line, cross-feed as triple dot-dashed brown lines, the combinatorial background as a long-dashed green line, and partially reconstructed background components with either a missing neutral pion as a dot-dashed purple line or a missing soft photon as a dotted cyan line.

predictions of *CP* violation in B mixing and also with small penguin contamination effects. BSM searches have been performed using FCNC $b \to sd\bar{d}$ and $b \to s\bar{s}s$ transitions where *CP* violation is expected to be close to zero in the SM. No *CP* violation is seen, though uncertainties are dominated by the limited dataset sizes. Preliminary analyses of FCNC transitions of beauty baryons have been performed, with first observations of the $\Lambda_b^0 \to \Lambda\phi$, $\Lambda_b^0 \to \Lambda K^+K^-$, and $\Lambda_b^0 \to K^+K^-$ decay modes reported. Measurements of *CP* violation in the form of direct *CP* asymmetries and triple product asymmetries are consistent with zero and will become very interesting with increased dataset sizes provided by Run II of the LHC.

References

1. J. Charles *et al.*, *Phys. Rev.* D **91**, 073007 (2015).
2. R. Aaij *et al.* [LHCb collaboration], *Phys. Rev. Lett.* **115**, 031601 (2015).
3. Y. Amhis *et al.*, arXiv:1412.7515 [hep-ph].
4. R. Aaij *et al.* [LHCb collaboration], *Phys. Rev. Lett.* **114**, 041801115 (2015).
5. A. Dighe *et al.*, *Eur. Phys. J.* C **6**, 647-662 (1999).
6. I. Dunietz *et al.*, *Phys. Rev.* D **63**, 114015 (2001).
7. J. Charles *et al.*, *Phys. Rev.* D **84**, 033005 (2011).
8. A. Lenz, *JHEP* **0706**, 072 (2007).
9. A. Lenz and U. Nierste, arXiv:1102.4274 [hep-ph].
10. P. Ball and R. Fleischer, *Eur. Phys. J.* C **48**, 413-426 (2006).
11. A. Lenz, *Phys. Rev.* D **76**, 065006 (2007).
12. R. Aaij *et al.* [LHCb collaboration], *JHEP* **06**, 131 (2015).
13. K. De Bruyn, R. Fleischer, *JHEP* **1503**, 145 (2015).
14. R. Aaij *et al.* [LHCb collaboration], *JHEP* **11**, 082114 (2015).
15. R. Aaij *et al.* [LHCb collaboration], *Phys. Lett.* B **742**, 38 (2015).
16. R. Aaij *et al.* [LHCb collaboration], *JHEP* **07**, 166 (2015).
17. M. Beneke *et al.*, *Nucl. Phys.* B **774**, 64-101 (2007).
18. H. Cheng and C. Chua, *Phys. Rev.* D **80**, 114026 (2009).
19. M. Gronau and J. Rosner, *Phys. Rev.* D **84**, 096013 (2011).
20. A. Datta *et al.*, arXiv:1207.4495 [hep-ph].
21. R. Aaij *et al.* [LHCb collaboration], *Phys. Rev.* D **90**, 052011 (2014).
22. R. Aaij *et al.* [LHCb collaboration], *Chin. Phys.* C **40**, 011001 (2015).
23. R. Aaij *et al.* [LHCb collaboration], LHCb-PAPER-2016-002, arXiv:1603.02870 [hep-ex].
24. O. Leitner and Z. J. Ajaltouni, Nucl. Phys. Proc. Suppl. 174 169 (2007).
25. R. Aaij *et al.* [LHCb collaboration], LHCb-PAPER-2016-004, arXiv:1603.00413 [hep-ex].